	A O S 1 2 3 0 4	WILEY	Dispatch: 15.10.13	Journal: AOS	CE: Liyagath Ali
	Journal Name Manuscript No.			No. of pages: 5	PE: Murugavel

A reproducible automated segmentation algorithm for corneal epithelium cell images from *in vivo* laser scanning confocal microscopy

Julien Bullet,[1] Thomas Gaujoux,[1] Vincent Borderie,[1] Isabelle Bloch[2] and Laurent Laroche[1]

[1]Institut de la Vision, Paris, France
[2]Telecom ParisTech - CNRS LTCI, Paris Cedex 13, France

ABSTRACT.

Purpose: **To evaluate an automated process to find borders of corneal basal epithelial cells in pictures obtained from *in vivo* laser scanning confocal microscopy (Heidelberg Retina Tomograph III with Rostock corneal module).**

Methods: **On a sample of 20 normal corneal epithelial pictures, images were segmented through an automated four-step segmentation algorithm. Steps of the algorithm included noise reduction through a fast Fourier transform (FFT) band-pass filter, image binarization with a mean value threshold, watershed segmentation algorithm on distance map to separate fused cells and Voronoi diagram segmentation algorithm (which gives a final mask of cell borders). Cells were then automatically counted using this border mask. On the original image either with contrast enhancement or noise reduction, cells were manually counted by a trained operator.**

Results: **The average cell density was 7722.5 cells/mm^2 as assessed by automated analysis and 7732.5 cells/mm^2 as assessed by manual analysis ($p = 0.93$). Correlation between automated and manual analysis was strong ($r = 0.974$ [0.934–0.990], $p < 0.001$). Bland–Altman method gives a mean difference in density of 10 cells/mm^2 and a limits of agreement ranging from −971 to +991 cells/mm^2. Visually, the algorithm correctly found almost all borders.**

Conclusion: **This automated segmentation algorithm is worth for assessing corneal epithelial basal cell density and morphometry. This procedure is fully reproducible, with no operator-induced variability.**

Key words: cell morphometry – corneal epithelium – image processing – *In vivo* laser scanning confocal microscopy

Acta Ophthalmol.

doi: 10.1111/aos.12304

Introduction

In vivo confocal microscopy allows taking pictures of selected corneal layers such as the corneal epithelium. Basal epithelial cells have a polygonal shape similar to that of corneal endothelial cells (Fig. 1). Analysis of epithelium basal cell morphology and density can help clinical and pathological diagnosis (Hu et al. 2008; Chen et al. 2009; Gaujoux et al. 2010). Recent publications show increasing interest in morphological analysis of basal epithelial cells, especially in limbal stem cell deficiency (Deng et al. 2012; Miri et al. 2012a).

The first step towards this analysis is to extract cell borders from a confocal image. A human operator drawing all cell borders often makes this task, called image segmentation, manually. However, this work can be time consuming, and it does not allow a large amount of data to be included for a statistical analysis process, inducing a bias. Furthermore, it is operator-dependent and may be poorly reproducible.

Julio et al. proposed, in 2008, a segmentation algorithm for corneal epithelial images obtained by transmission electron microscopy. Bandekar et al. in 2011, developed an automated cell counting technique for *ex vivo* epithelial cell images. However, these images are very different from confocal images.

Endothelial cells have a similar polygonal shape, and several automated cell count algorithms have been proposed for assessing the endothelial cell density. Contrast-based segmentation methods were initially proposed by Lester et al. in 1978 and 1981, and other algorithms

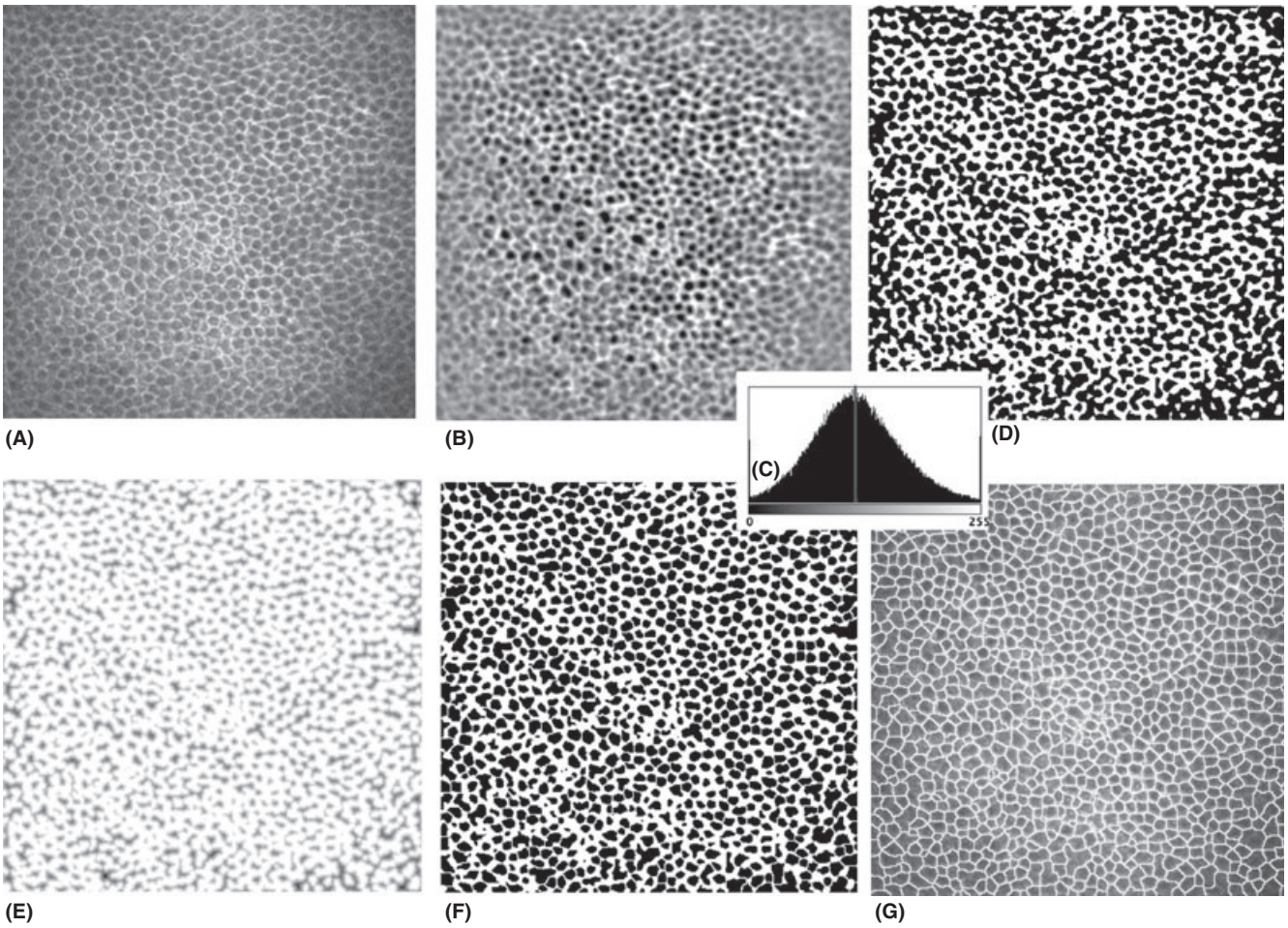

Fig. 1. Steps of the algorithm. (A) A normal corneal basal cell epithelium viewed through an *in vivo* confocal microscope (Heidelberg Retina Tomograph with Rostock corneal module). (B) Same image after FFT band-pass filter and normalization. (C) Grey-level histogram with mean value. (D) Results of image binarization. (E) Distance map (grey levels are here inverted to allow a reasonable printing). (F) Separation results after watershed algorithm. (G) Result of Voronoi segmentation pasted on original image.

combining threshold binarization and simple morphological transformations have been proposed afterwards (Hartmann & Köditz 1984; Hirst et al. 1984; Nishi & Hanasaki 1988; Corkidi et al. 1993; Siertsema et al. 1993). More sophisticated algorithms have been developed such as Sanchez-Martin 'unsharp masking'-based algorithm (Sanchez-Marin 1999) or Vincent & Masters morphological geodesic reconstruction in 1992. Khan et al. published a wavelet-based approach to segmentation in 2007, and Gain et al. (2002) performed a segmentation of endothelial cells on three images to increase sample size. But, once again, images are very different, especially cell size and contrast which is inverted.

We propose here a different, fully automated approach, which has been adapted to basal epithelial cell confocal images.

Material and Methods

Confocal images

Corneal confocal images of 20 eyes from 20 patients with healthy corneal epithelium were used. Characteristics of patients and eyes have been reported previously (Gaujoux et al. 2010). All patients firmed an informed consent and local ethical committee was consulted.

Confocal pictures were taken using the Heidelberg Retina Tomograph III with the Rostock Cornea Module (HRT III/RCM; Heidelberg Engineering GmbH, Heidelberg, Germany). Images consisted of 384 × 384 pixels covering an area of 300 × 300 μm with transversal optical resolution of approximately 0.78 micrometre per pixel and an acquisition time of 0.024 seconds.

Image analysis

We used NIH ImageJ free software (version 1.43u) with implementation of all functions. A single picture considered as having a good quality of basal cell layer was selected for each patient (size 300 × 300 μm, 384 × 384 pixels). In each picture, a 200 × 100 μm (256 × 128 pixels) frame was selected before segmentation. On this frame, manual and automated counts were performed. This sample allowed at least 75 cells to be counted.

Automated cell count was achieved through a 4-step fully automated segmentation process (Fig. 1):

- Noise reduction through a fast Fourier transform (FFT) band-pass filter with normalization (pixel values range from 0 to 255). This step eliminated low- and high-spatial frequency noise (below 3 pixels and

above 40 pixels). FFT transformed original picture to a two-dimensional representation of its frequencies. A simple mask was applied. It reduced frequency coefficients below a low threshold and above a high threshold to zero and suppresses those frequencies in the picture. A reverse FFT moved back to the modified original picture. All these steps were performed at once using 'Process > FFT > Bandpass Filter…' function in ImageJ.

- Image binarization with a mean value threshold. Mean value could easily be found on grey level histogram. All pixels with a lower than the threshold value were set to 0 (black), all other pixels are set to 1 (white). Binarized image contained round cell markers. These markers were sometimes fused together in a rosary fashion.
- Standard watershed algorithm on distance map was used to separate fused markers. Two steps were carried out at once using 'Process > Binary > Watershed' ImageJ function. First, a distance map was computed: every pixel value in the binary picture was replaced by its distance to the nearest white point. This produced a grey-level image where all marker centres were clearer. Watershed algorithm, a usual image processing segmentation algorithm (Beucher & Lantuéjoul 1979; Beucher & Meyer 1993), was then applied to distance picture. Considering this picture as a topographic map with grey level indicating altitude, there were mounts and valleys in the picture. Watershed defined water catchment areas in the map, as water flows from highest points to valleys. This algorithm finds frontiers between these catchment areas. From the original binary marker pictures, fused rosary markers are thus separated by these frontiers.
- Voronoi diagram segmentation algorithm gave a final polygonal border map. Cells borders are found by drawing a line of equidistant points between every couple of marker centre. Those lines formed a polygon around every centre and represent cell borders.

After performing segmentation in each picture, cells were automatically counted using 'Analyse>Analyse Particles…' function in ImageJ.

A first count excluded all cells on the border. A second count included them, and a mean count was calculated. Density was evaluated by dividing a mean of those two counts by a $0.1 \times 0.2\ \mu m^2$ surface.

Cells were manually counted to compare with automated segmentation. A single operator counted cells in the $200 \times 100\ \mu m$ frames selected from confocal pictures by pointing on cell centre. No software was used except when contrast in original images between cells and borders was too low. Operator could then use a normalized noise-reduced image. This image was obtained using algorithm's first step with a FFT band-pass filter.

As with automated count method, a first count established a number of inside cells by excluding those on the border. A second count of border cells on one small and one large border of the picture was added to give a final reference cell count. Density was evaluated by dividing this count by a $0.1 \times 0.2\ \mu m^2$ surface.

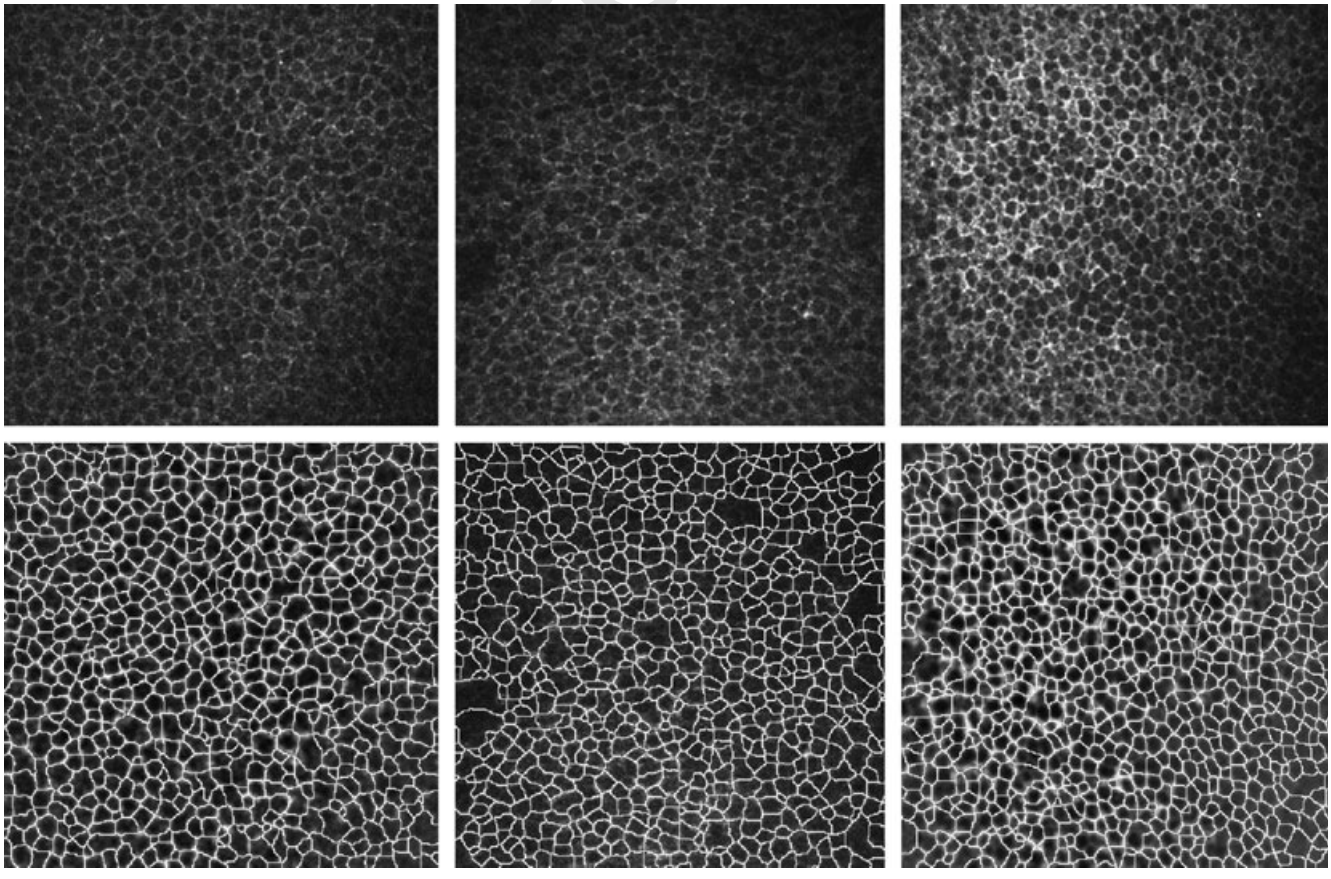

Fig. 2. Several images fused with their segmentation results after applying segmentation algorithm.

Statistical analysis

Normality of distribution of both automated and manual cell counts and densities was assessed by a Kolmogorov–Smirnov test, and both populations were respectively compared using a Student's *t*-test. Pearson correlation between normal and automated populations was calculated.

We used Statistica 6.1 by Statsoft France, Maisons-Alfort, France.

Results

Segmentation results were correct (Fig. 2), although imperfect. Most cell borders were correctly found. Some cells were over segmented with unreal borders being drawn, some other subsegmented with several cells being fused together in one. However, these effects were marginal and they affected only very few zones in images and a low number of cells.

Operator requested the use of normalized noise-reduced images for only 1 of 20 pictures (5%). This image had a real low contrast and low grey levels that did not allow an easy manual count. Results were similar between manual and automated cell count and density (Table 1) with a mean relative error rate of 5% (1–10%). No image had a relative density error >10%.

Pearson correlation coefficient between automated and manual density was 0.974 (0.934–0.990), $p < 0.001$ (Fig. 3).

With cells densities ranging from 5000 to 11 000 cells/mm^2, Bland–Altman method gives a mean difference in density of 10 cells/mm^2 and a limits of agreement from – 971 to +991 cells/mm^2 (Fig 4).

Automated segmentation process allowed us to find cell morphometric characteristics as mean area, perimeter, circularity and Feret diameter (Table 1).

Discussion

Pictures from laser scanning confocal microscopy allow *in vivo* morphological analysis of basal epithelial cells. Recent publications show an increasing interest in this technique. However, analysis is currently performed either manually on a small set of randomly selected cells as in Leonardi et al. (2012) or on the whole cornea with

Table 1. Results from manual and automated cell counts and density with relative error and morphometric cell characteristics (20 images).

	Mean	Interval	
Manual count MC	154.65	102	230
Automated count AC	154.45	86	186
Manual density	7732.5	5100	11500
Automated density	7722.5	5550	10900
Relative error	5%	1%	10%
Mean cell area	102.3	67.5	148.1
Mean cell perimeter	39.3	32.0	48.0
Mean circularity	0.79	0.77	0.807
Mean Feret diameter	14.6	12.2	17.5

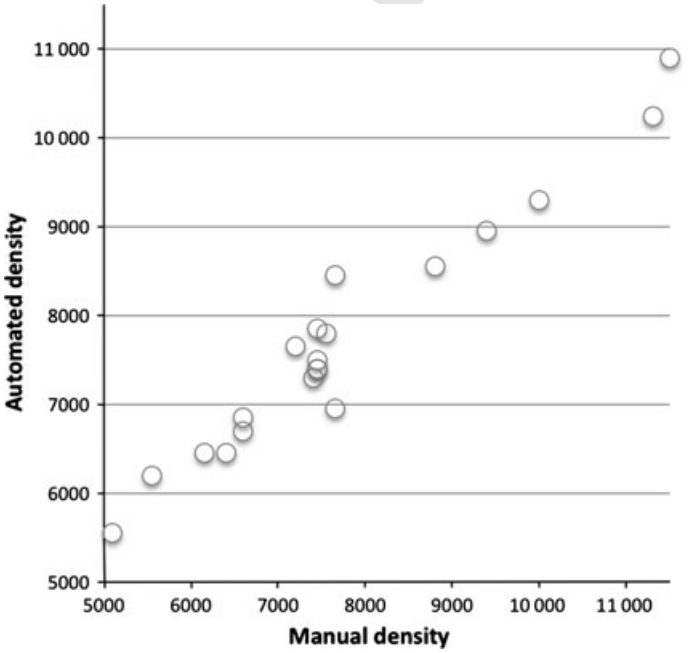

Fig. 3. Automated and manual cell density representation showing high correlation.

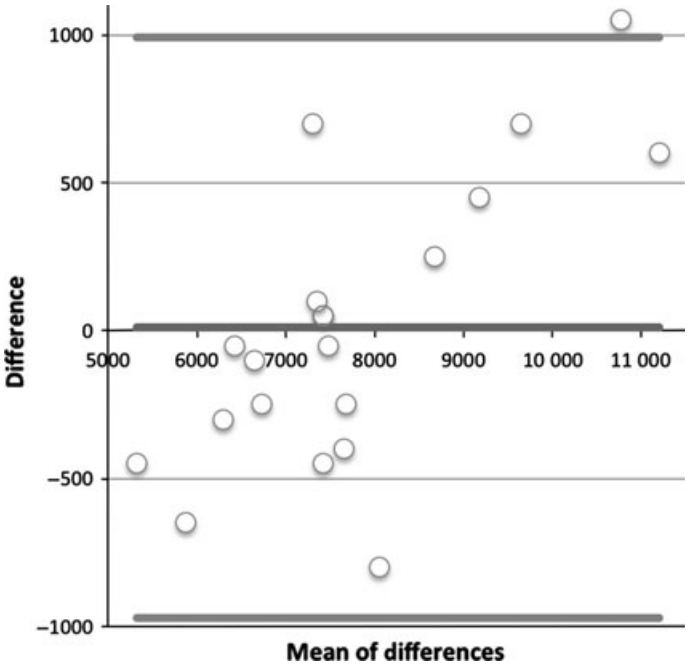

Fig. 4. Bland–Altman graphic with mean difference and limits of agreement.

the help of an image software as in Deng et al. (2012) and Miri et al. (2012a,b)with the user manually finding characteristics.

Algorithm proposed for epithelial cell segmentation (Julio et al. 2008; Bandekar et al. 2011) was applied to images very different from confocal images. Transmission electron microscopy has a much higher resolution, and *ex vivo* cell samples were acquired for the purpose of studying the side-effects of lens wear and lens cleaning solutions on human corneal epithelial cells, collecting only few cells. Although not tested, it is very unlikely that algorithms created for the analysis of different type of images might work on confocal images. To the best of our knowledge, no specific segmentation algorithm has been developed for *in vivo* laser scanning confocal microscopy of basal epithelial cell. However, use of a user-independent, fully reproducible method could be helpful for researchers interested in the topic.

Confocal microscopy images of corneal epithelium can be segmented because these pictures contain a high number of small cells with good contrast between dark cell cytoplasm and cell white borders. This contrast is very important for algorithm robustness. The first way to segment images is to use a simple threshold, as carried out in step 2. However, threshold methods do not give reliable results with noisy images. Reducing noise level is very important before using a threshold method.

Residual noise leads to fused markers after step 2. Without separation, a group of fused markers would lead to a single cell found at final step. Luckily, the watershed algorithm, a powerful usual segmentation algorithm, can solve the problem: all markers are fused in a rosary fashion, that is, with a connecting zone less wide than markers themselves (Fig. 1D). On distance map, this appears as a 'ridge line' and also a frontier between two catchment basins in the watershed algorithm.

Once markers are correctly segmented, Voronoi diagram finds almost all cell borders correctly. Some borders might be deviated from their real position, but this affects only very few cells in the picture. Furthermore, it respects the polygonal shape of epithelial basal cells.

All pictures considered for this work originated from normal corneal epithelia. However, we are currently testing it on cornea with pathological modifications.

As a conclusion, the use of an automated segmentation process could allow more data to be analysed, more morphologic characteristics to be considered when looking for diagnostic criteria, and relieve bias in analysis with little variation in measure and a greater reproducibility.

Acknowledgements

An abstract of this work has been previously reported at American Research in Vision and Ophthalmology annual meeting 2011, Fort Lauderdale, Florida, USA.

Conflict of Interest

No conflict of interest.

References

Bandekar N, Wong A, Clausi D & Gorbet M (2011): A novel approach to automated cell counting for studying human corneal epithelial cells. Conf Proc IEEE Eng Med Biol Soc **2011**: 5997–6000.

Beucher S & Lantuéjoul C (1979): Use of watersheds in contour detection.

Beucher S & Meyer F (1993): The morphological approach to segmentation: the watershed transformation. In: Dougherty ER (ed.). Mathematical morphology in image processing mathematical morphology in image processing. ???????: ??????? 433–481.

Chen JJ, Rao K & Pflugfelder SC (2009): Corneal epithelial opacity in dysfunctional tear syndrome. Am J Ophthalmol **148**: 376–382.

Corkidi G, Marquez J, Usisima R, Toledo R, Valdéz J & Graue E (1993): Automated *in vivo* and online morphometry of human corneal endothelium. Med Biol Eng Comput **31**: 432–437.

Deng SX, Sejpal KD, Tang Q, Aldave AJ, Lee OL & Yu F (2012): Characterization of limbal stem cell deficiency by *in vivo* laser scanning confocal microscopy: a microstructural approach. Arch Ophthalmol **130**: 440–445.

Gain P, Thuret G, Kodjikian L et al. (2002): Automated tri-image analysis of stored corneal endothelium. Br J Ophthalmol **86**: 801–808.

Gaujoux T, Touzeau O, Laroche L & Borderie VM (2010): Morphometry of corneal epithelial cells on normal eyes and after anterior lamellar keratoplasty. Cornea **29**: 1118–1124.

Hartmann C & Kŏditz W (1984): Automated morphometric endothelial analysis combined with video specular microscopy. Cornea **3**: 155–167.

Hirst LW, Sterner RE & Grant DG (1984): Automated analysis of wide-field specular photomicrographs. Cornea **3**: 83–87.

Hu Y, Matsumoto Y, Adan ES, Dogru M, Fukagawa K, Tsubota K & Fujishima H (2008): Corneal *in vivo* confocal scanning laser microscopy in patients with atopic keratoconjunctivitis. Ophthalmology **115**: 2004–2012.

Julio G, Merindano MD, Canals M & Ralló M (2008): Image processing techniques to quantify microprojections on outer corneal epithelial cells. J Anat **212**: 879–886.

Khan M, Khan K, Khan A & Ibrahim T (2007): Endothelial cell image enhancement using non-subsampled image pyramid. Inf Technol J **6**: 1057–1062.

Leonardi A, Lazzarini D, Bortolotti M, Piliego F, Midena E & Fregona I (2012): Corneal confocal microscopy in patients with vernal keratoconjunctivitis. Ophthalmology **119**: 509–515.

Lester JM, Williams HA, Weintraub BA & Brenner JF (1978): Two graph searching techniques for boundary finding in white blood cell images. Comput Biol Med **8**: 293–308.

Lester JM, McFarland JL, Bursell SE, Laing RA & Brenner JF (1981): Automated morphometric analysis of corneal endothelial cells. Invest Ophthalmol Vis Sci **20**: 407–410.

Miri A, Al-Aqaba M, Otri AM, Fares U, Said DG, Faraj LA & Dua HS (2012a): *In vivo* confocal microscopic features of normal limbus. Br J Ophthalmol **96**: 530–536.

Miri A, Alomar T, Nubile M et al. (2012b): *In vivo* confocal microscopic findings in patients with limbal stem cell deficiency. Br J Ophthalmol **96**: 523–529.

Nishi O. & Hanasaki K. (1988): Automated morphometry of corneal endothelial cell: use of video camera and video tape recorder. Br J Ophthalmol **72**: 68–73.

Sanchez-Marin FJ (1999): Automatic segmentation of contours of corneal cells. Comput Biol Med **29**: 243–258.

Siertsema JV, Landesz M, van den Brom H & van Rij G. (1993): Automated video image morphometry of the corneal endothelium. Doc Ophthalmol **85**: 35–44.

Vincent L & Masters B. (1992): Morphological image processing and network analysis of corneal endothelial cell images. Proc. SPIE **1769**: 212–226.

Received on June 3rd, 2012.
Accepted on October 2nd, 2013.

Correspondence:
Julien Bullet
Institut de la Vision
17, rue Moreau
Paris 75012
France
Tel: + 33 1 40 02 15 04
Fax: + 33 1 40 02 15 99
Email: jbullet@quinze-vingts.fr

Author Query Form

Journal: AOS
Article: 12304

Dear Author,
During the copy-editing of your paper, the following queries arose. Please respond to these by marking up your proofs with the necessary changes/additions. Please write your answers on the query sheet if there is insufficient space on the page proofs. Please write clearly and follow the conventions shown on the attached corrections sheet. If returning the proof by fax do not write too close to the paper's edge. Please remember that illegible mark-ups may delay publication. Many thanks for your assistance.

Query reference	Query	Remarks
1	**AUTHOR: Vincent et al. (1992) has been changed to Vincent and Masters (1992) so that this citation matches the Reference List. Please confirm that this is correct.**	
2	**AUTHOR: Gain et al. has been changed to Gain et al. 2002 so that this citation matches the Reference List. Please confirm that this is correct.**	
3	**AUTHOR: Please give manufacturer information for NIH ImageJ free software (version 1.43u): company name, town, state (if USA), and country.**	
4	**AUTHOR: More than one reference shares the same author and year-of-publication details. Please check that they have been correctly differentiated between using a, b, etc. after the year of publication.**	
5	**AUTHOR: Please provide missing information for reference Beucher and Lantuéjoul (1979).**	
6	**AUTHOR: Please provide the publisher name, publisher location for reference Beucher and Meyer (1993).**	

USING e-ANNOTATION TOOLS FOR ELECTRONIC PROOF CORRECTION

Required software to e-Annotate PDFs: Adobe Acrobat Professional or Adobe Reader (version 8.0 or above). (Note that this document uses screenshots from Adobe Reader X)
The latest version of Acrobat Reader can be downloaded for free at: http://get.adobe.com/reader/

Once you have Acrobat Reader open on your computer, click on the Comment tab at the right of the toolbar:

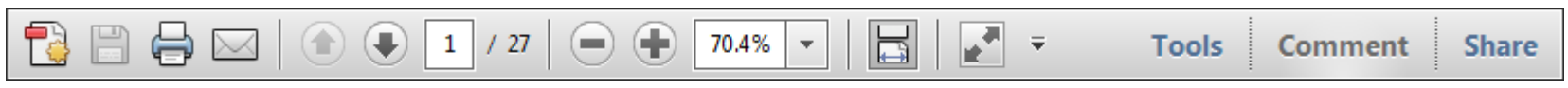

This will open up a panel down the right side of the document. The majority of tools you will use for annotating your proof will be in the Annotations section, pictured opposite. We've picked out some of these tools below:

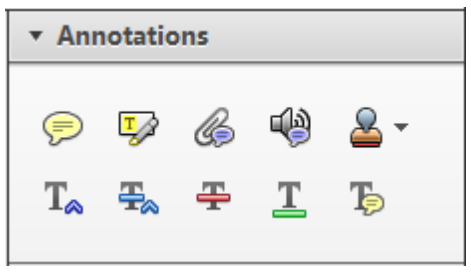

1. Replace (Ins) Tool – for replacing text.

Strikes a line through text and opens up a text box where replacement text can be entered.

How to use it

- Highlight a word or sentence.
- Click on the Replace (Ins) icon in the Annotations section.
- Type the replacement text into the blue box that appears.

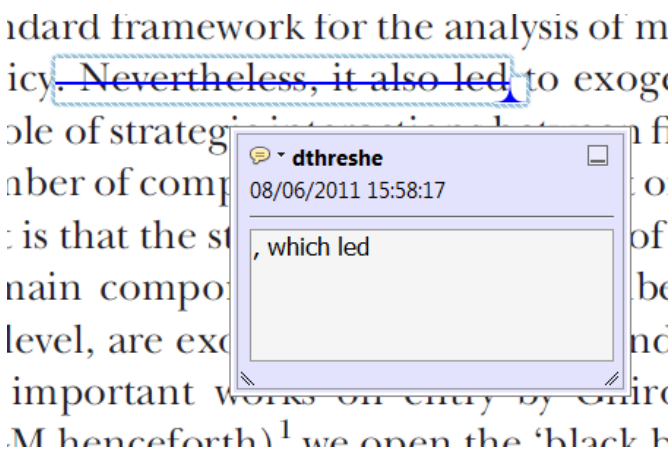

2. Strikethrough (Del) Tool – for deleting text.

Strikes a red line through text that is to be deleted.

How to use it

- Highlight a word or sentence.
- Click on the Strikethrough (Del) icon in the Annotations section.

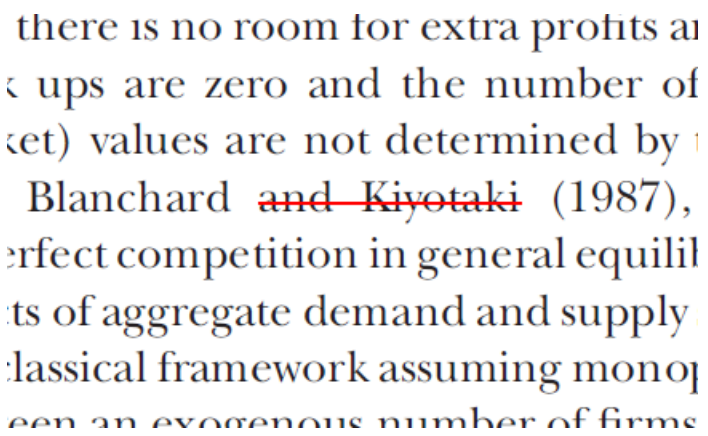

3. Add note to text Tool – for highlighting a section to be changed to bold or italic.

Highlights text in yellow and opens up a text box where comments can be entered.

How to use it

- Highlight the relevant section of text.
- Click on the Add note to text icon in the Annotations section.
- Type instruction on what should be changed regarding the text into the yellow box that appears.

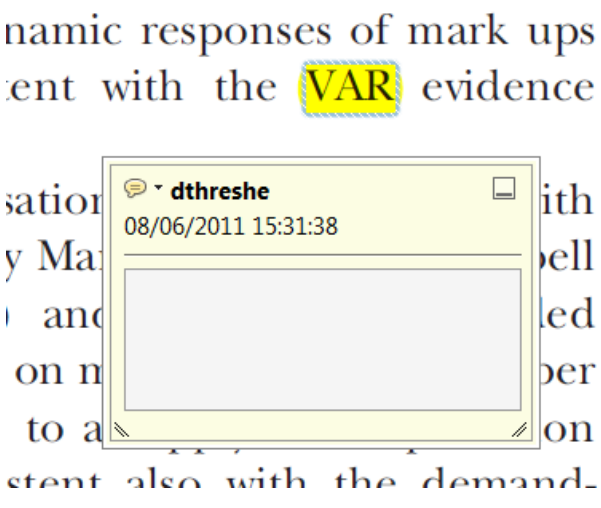

4. Add sticky note Tool – for making notes at specific points in the text.

Marks a point in the proof where a comment needs to be highlighted.

How to use it

- Click on the Add sticky note icon in the Annotations section.
- Click at the point in the proof where the comment should be inserted.
- Type the comment into the yellow box that appears.

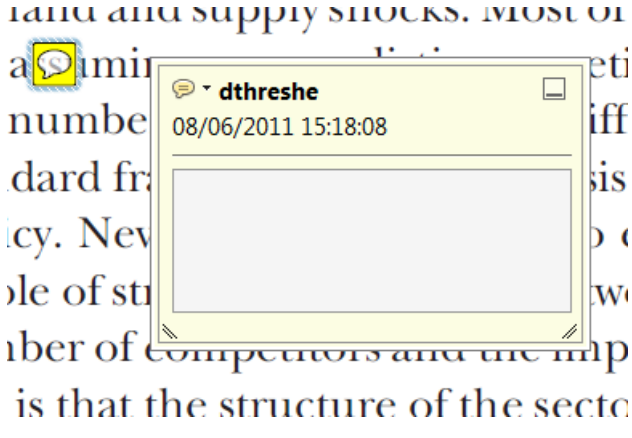

WILEY-BLACKWELL

USING e-ANNOTATION TOOLS FOR ELECTRONIC PROOF CORRECTION

5. Attach File Tool – for inserting large amounts of text or replacement figures.

Inserts an icon linking to the attached file in the appropriate pace in the text.

How to use it

- Click on the Attach File icon in the Annotations section.
- Click on the proof to where you'd like the attached file to be linked.
- Select the file to be attached from your computer or network.
- Select the colour and type of icon that will appear in the proof. Click OK.

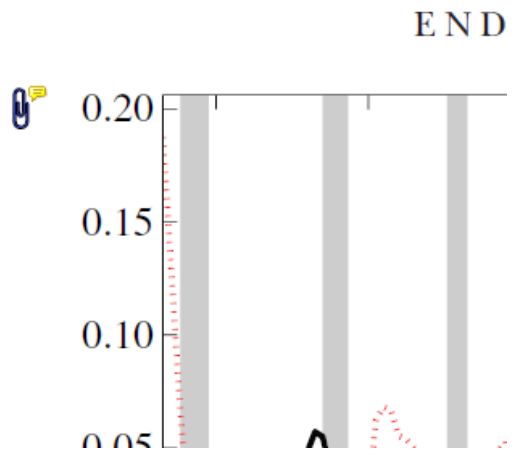

6. Add stamp Tool – for approving a proof if no corrections are required.

Inserts a selected stamp onto an appropriate place in the proof.

How to use it

- Click on the Add stamp icon in the Annotations section.
- Select the stamp you want to use. (The Approved stamp is usually available directly in the menu that appears).
- Click on the proof where you'd like the stamp to appear. (Where a proof is to be approved as it is, this would normally be on the first page).

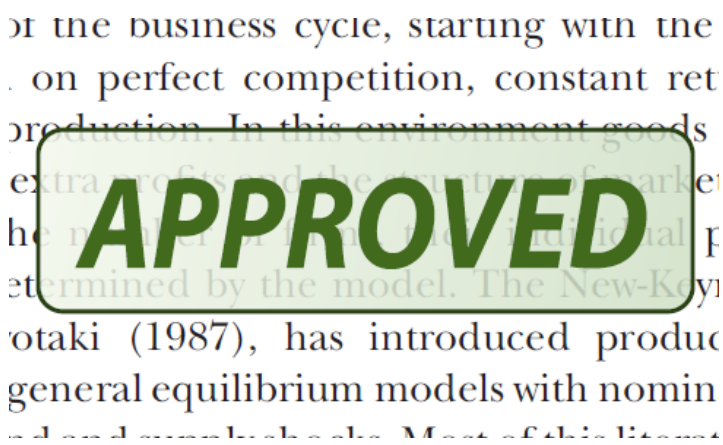

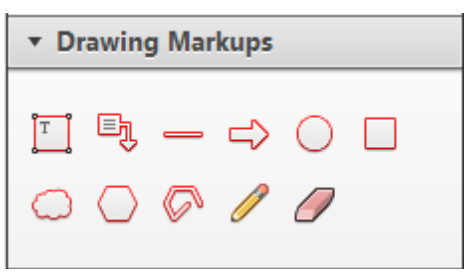

7. Drawing Markups Tools – for drawing shapes, lines and freeform annotations on proofs and commenting on these marks.

Allows shapes, lines and freeform annotations to be drawn on proofs and for comment to be made on these marks..

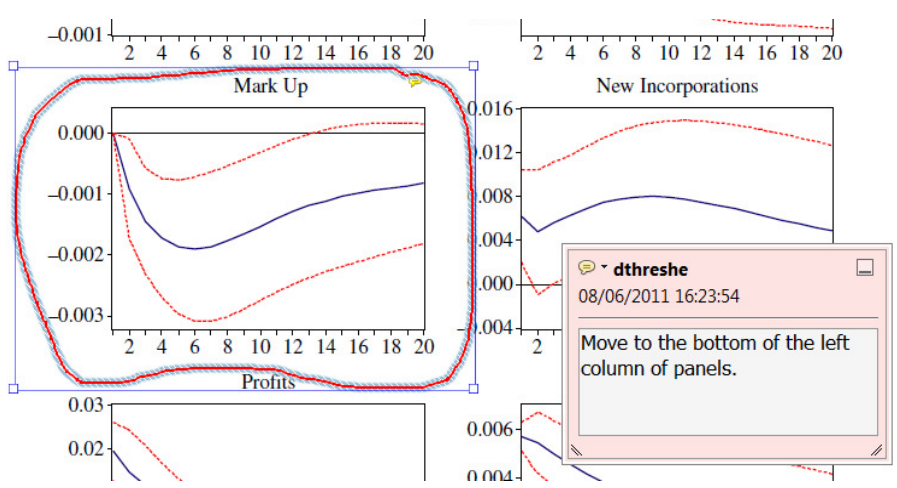

How to use it

- Click on one of the shapes in the Drawing Markups section.
- Click on the proof at the relevant point and draw the selected shape with the cursor.
- To add a comment to the drawn shape, move the cursor over the shape until an arrowhead appears.
- Double click on the shape and type any text in the red box that appears.

For further information on how to annotate proofs, click on the Help menu to reveal a list of further options: